Supramolecular Chemistry
Publication details, including instructions for authors and subscription information:
http://www.tandfonline.com/loi/gsch20

Synthesis, crystal structure and DNA interaction studies of a 2D cadmium(II) coordination polymer constructed from 2-(2-pyridyl)benzimidazole

Yan Yang[a], Chang-Gui Li[b], Xu-Jian Luo[a], Zhi-Hui Luo[a], Rong-Jun Liu[a], Yue-Xiu Jiang[b] & Wei-Jiang Liang[a]

[a] School of Chemistry and Material, Yulin Normal University, Yulin537000, P.R. China

[b] School of Chemistry and Chemical Engineering, Guangxi University, Nanning530004, P.R. China

Published online: 24 Sep 2014.

Supramolecular Chemistry, 2015
Vol. 27, No. 4, 281–286, http://dx.doi.org/10.1080/10610278.2014.959015

Synthesis, crystal structure and DNA interaction studies of a 2D cadmium(II) coordination polymer constructed from 2-(2-pyridyl)benzimidazole

Yan Yang[a]*, Chang-Gui Li[b], Xu-Jian Luo[a], Zhi-Hui Luo[a], Rong-Jun Liu[a], Yue-Xiu Jiang[b]* and Wei-Jiang Liang[a]*

[a]*School of Chemistry and Material, Yulin Normal University, Yulin 537000, P.R. China;* [b]*School of Chemistry and Chemical Engineering, Guangxi University, Nanning 530004, P.R. China*

(*Received 20 June 2014; accepted 25 August 2014*)

A new complex associated with Cd^{2+}, $[Cd(OH\text{-}H_2Bdc)(2\text{-}Pbim)]_n$ (**1**), ($OH\text{-}H_2Bdc$ = 5-hydroxyisophthalic acid, 2-Pbim = 2-(2-pyridyl)benzimidazole), has been synthesised under hydrothermal conditions and characterised by elemental analysis, FT-IR spectroscopy, TG/DTG and fluorescence spectrum. Its *in vitro* cytotoxicity towards four selected tumour cell lines has been evaluated by an microculture tetrozolium assay, the results suggest that complex **1** displays greater inhibition than the free benzimidazole ligand. On the basis of the combination of absorption titration and fluorescence emission titration, the binding mode of complex **1** to calf thymus DNA has been investigated. Complex **1** can interact with the base pairs of double-helical DNA via the combined mode of intercalation and groove binding with larger binding constants.

Keywords: cadmium(II) complex; crystal structure; fluorescent property; DNA interaction

Introduction

The interaction of transition metal complexes with DNA has been extensively studied for their use as probes for DNA structure and their potential applications in molecular light switches, DNA footprinting agents, nucleic acid probes, chemotherapy and photodynamic therapy (*1–3*). One of the most important DNA related activities of the transition metal complexes is that some of the complexes show the ability to insert DNA (*4*). Structures containing benzimidazole, well-known to have a wide range of biological properties, have commercial applications in various realms of therapy, including antiulcerative, antihypertensive, antiviral, antifungal, anti-tumour and antihistaminic agents, and antihelminthic agents in veterinary medicine (*5*). So we begin to study the 2-(2-pyridyl) benzimidazole (Pbim). In fact, as a chelate ligand Pbim has multiple coordination modes in forming metal coordination polymers. It can chelate not only as a capping ligand but also as a bridging ligand when it is deprotonated (*6–8*), which is different from the benzimidazole ligand (*9*). As a rigid and versatile bridging, 5-hydroxyisophthalic acid has been extensively studied for designing a new coordination polymer because its two carboxylic groups can bond with metal centres and the hydroxyl group, an electron-withdrawing group coexisting in isophthalic acid, can not only act as a hydrogen bond acceptor, but also exhibit steric effects (*10*, *11*). We have reported some complexes (*12–14*) in recent years. Herein, we report the synthesis, characterisation and DNA interaction of $[Cd(OH\text{-}H_2Bdc)(2\text{-}Pbim)]_n$ (1) ($OH\text{-}H_2Bdc$ = 5-hydroxyisophthalic acid, 2-Pbim = 2-(2-pyridyl)benzimidazole). Its *in vitro* cytotoxicity towards four selected tumour cell lines has been evaluated by the microculture tetrozolium (MTT) (3-[4,5-dimethylthiazol-2-yl]-2,5-diphenyltetrazolium bromide) method. The combination of absorption titration and fluorescence emission titration has been used to study the interaction of this compound with DNA.

Experimental

Materials and methods

All reagents were bought from commercial sources and used without further purification. IR spectra were recorded in the range 4000–400 cm^{-1} on Perkin–Elmer Spectrum One FT/IR spectrometer using a KBr pellet. Elemental analysis (C, H, N) was performed on a Perkin–Elemer 2400II CHN elemental analyser. TGA (thermogravimetric analysis) was recorded on Perkin–Elmer Pyris Diamond TG/DTA analyser. Emission spectra were measured on Ls55 spectrofluorophotometer (Horiba Jobin Jvon, France). UV–vis absorption titration was performed on a Cary 100 Conc. UV–vis spectrophotometer (Agilent Technologies, Australia). Fluorescence emission titration was performed on a Shimadzu RF-5301/PC spectrofluorometer (Tianmei Technologies, Japan). The crystal structure was determined by a Bruker APEX area-detector diffractometer (Bruker, Germany) and employing the SHELXTL crystallographic software. Calf thymus DNA (CT-DNA) was purchased from Sigma. Buffer (5 mM tris(hydroxymethyl)aminomethane (Tris) hydrochloride, 50 mM NaCl, pH 7.35) was used for

*Corresponding authors. Email: yy135175@163.com; gxu2110@163.com; liang2179@163.com

emission titration experiments. The concentration of CT-DNA was determined spectrophotometrically assuming a molar absorption of 6600 M^{-1} cm^{-1} (260 nm) (*15–16*). The emission titration of the complex was performed by using a fixed complex concentration to which increments of the DNA stock solution were added. The concentration of complex solution was 10^{-6} M. Complex–DNA solutions were allowed to incubate for 10 min before the emission spectra were recorded.

Synthesis of [Cd(OH-H_2Bdc)(2-Pbim)]$_n$ (1)

A solution of 2-Pbim (0.5 mmol) and 5-hydroxyisophthalic acid (0.5 mmol) in acetonitrile (10 mL) was added to water solution (5 mL) of $Cd(NO_3)_2{\cdot}4H_2O$ (1 mmol). The mixture was stirred for 30 min, and then 0.6 mL triethylamine was added. The mixture was placed in a 23 mL Teflon-lined autoclave and heated at 140°C for 5 days and then cooled to room temperature. Colourless crystals were obtained (yield 19% based on OH-H_2Bdc), filtered off, washed with distilled water and dried in air. Elemental analysis (%): Anal. calcd C, 49.25; H, 2.69; N, 8.62; found C, 49.09; H, 2.92; N, 8.57. IR (KBr, cm^{-1}): v = 3422, 3252, 3087, 1596, 1547, 1525, 1478, 1451, 1437, 1391, 1322, 1297, 1207, 1138, 1119, 1053, 976, 795, 743, 620.

X-ray diffraction experiment

Diffraction data were collected on a Bruker Smart Apex CZN diffractometer with graphite-monochromated MoKα radiation (λ = 0.71073 Å) at 296 K. Absorption correction was applied by SADABS (*17*). The structure was solved by direct methods and refined with full-matrix least-squares technique using SHELXTL (*18*). All non-hydrogen atoms were refined with anisotropic displacement parameters. The crystal data, details on the data collection and refinement are summarised in Table 1, and selected bond lengths and angles are presented in Table 2. The hydrogen bond lengths (nm) and bond angles (°) are listed in Table 3. Figures 1–4 illustrate the structure of **1**.

Cytotoxicity assay

Cell lines: MDA-MB-231, A549, HeLa and MG-63 were obtained from the Shanghai Cell Bank in the Chinese Academy Sciences. Tumour cell lines were grown in PPMI-1640 medium supplemented with 10% (v/v) foetal bovine serum, 2 mM glutamine, 100 U/mL penicillin and 100 U/mL streptomycin at 37°C, in a highly humidified atmosphere of 95% air/5% CO_2. The cytotoxicity of MT and complex **1** against MDA-MB-231, A549, HeLa and MG-63 cell lines was examined by the MTT assay (*19*). The experiments were carried out using reported procedure (*20*). The growth inhibitory rate of treated cells was calculated using the data from three replicate tests by $(OD_{control}-OD_{test})/OD_{control}\times 100\%$. The complex was incubated with cell lines, respectively, for 24, 48 and 72 h with concentration gradient of 3.125, 6.25, 12.5, 25 and 50 μg/mL.

Table 1. Crystal data and structure refinement for **1**.

Empirical formula	$C_{20}H_{13}N_3O_5Cd$
Formula weight	487.75
Temp (K)	296(2)
Crystal system	Monoclinic
Space group	$P2_1/c$
a (Å)	10.577(4)
b (Å)	10.037(4)
c (Å)	17.369(6)
α (°)	90
β (°)	97.717(4)
γ (°)	90
V (Å^3)	1827.2(12)
Crystal size (mm)	0.20 × 0.25 × 0.30
Z	4
D_c (g cm^{-3})	1.773
μ (cm)	12.3
F(0 0 0)	968
Limiting indices	$-10 \le h \le 13$
	$-12 \le k \le 12$
	$-21 \le l \le 19$
Reflections	10151
Independent	3566
Observed data	3201
Npar	262
R_{int}	0.02
GOF	1.17
R_1^a ($I > 2\sigma(I)$)	0.0471
wR_2^a(all data)	0.0908
Max/min electron density (e Å^{-3})	1.14/−1.12
θ range (°)	2.3, 26.0

Table 2. Selected bond lengths (Å) and bond angles (°) for **1**.

Zn(1)–O(1)	2.264(3)	Zn(1)–N(1)	2.146(3)
Zn(1)–O(2)	2.068(2)	Zn(1)–N(3)	2.046(3)
Zn(1)–O(3)	1.984(3)		
O(1)–Zn(1)–O(2)	60.59(9)	O(2)–Zn(1)–C(15)	30.76(11)
O(1)–Zn(1)–O(3)	89.64(9)	O(3)–Zn(1)–N(1)	96.33(10)
O(1)–Zn(1)–N(1)	171.05(10)	O(3)–Zn(1)–N(3)	144.45(12)
O(1)–Zn(1)–N(3)	98.36(9)	O(3)–Zn(1)–C(15)	93.38(10)
O(1)–Zn(1)–C(15)	30.09(10)	N(1)–Zn(1)–N(3)	80.62(10)
O(2)–Zn(1)–O(3)	101.40(11)	N(1)–Zn(1)–C(15)	142.23(12)
O(2)–Zn(1)–N(1)	111.48(11)	N(3)–Zn(1)–C(15)	110.73(10)
O(2)–Zn(1)–N(3)	112.74(11)		

[a]Symmetry code: (a) $-x, -1/2+y, 1/2-z$; (d) $x, 3/2-y, -1/2+z$.

Table 3. Distances (Å) and angles (°) of hydrogen bonds for **1**.

D–H···A	d(D–H)	d(H···A)	d(D···A)	<(D–H···A)
N3–H3···O4[a]	0.8601	1.9565	2.735(5)	149.91
O5–H5···O1[b]	0.8198	1.9033	2.690(5)	160.56
C1–H1···O3[c]	0.9309	2.5787	3.163(7)	121.26
C8–H8···O1	0.9304	2.3670	3.160(7)	142.96

Notes: Symmetry code: (a) $1-x,-1/2+y,1/2-z$; (b) $-x,-1/2+y,1/2-z$; (c) $-x,-1/2+y,1/2-z$.

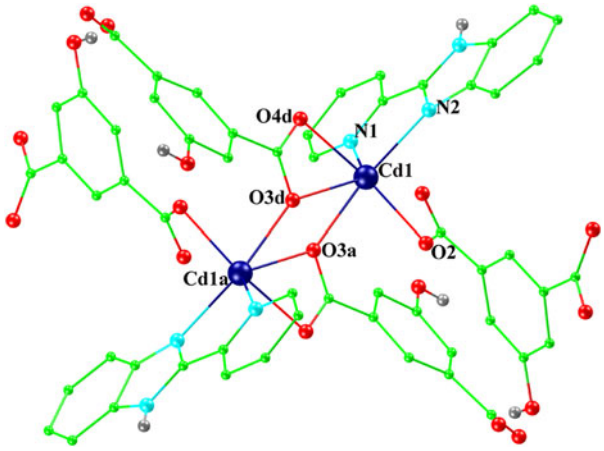

Figure 1. (Colour online) Coordination environment of Cd(II) metal ion in **1**.

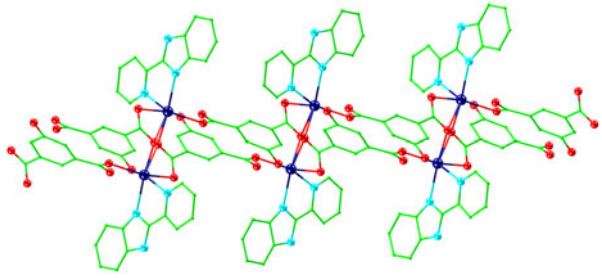

Figure 2. (Colour online) 1D ladder chain in **1** along *b* axis.

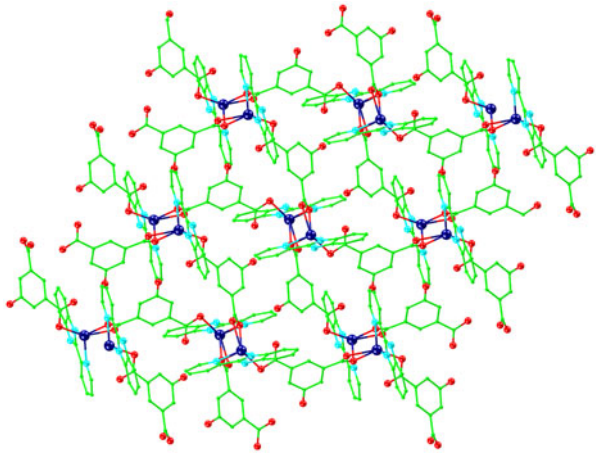

Figure 3. (Colour online) 2D structure of **1** along *bc* plane.

Crystal structure of 1

Single-crystal X-ray diffraction studies performed on a block of colourless crystals of **1** reveal the presence of a 2D layer constructed from 1D ladder chains running along the crystallographic *b* direction. In the asymmetric unit there is one unique Cd atom that is bridged by carboxylate groups from Bdc ligand and two N atoms of 2-Pbim ligands to give a distorted octahedral coordination environment (Figure 1). In the coordination network of **1**, the Cd(II) atoms occur in pairs and are bridged by a μ_2–COO^-. Each pair of Cd(II) atoms is connected by a Bdc ligand with 1D ladder chains (Figure 2). In the structure, the Bdc ligand adopts μ_3-bridging coordination fashion: one carboxylate group adopts chelating/bridging mono-bidentate coordination mode to connect the Cd(II) centres, and another carboxylate group acts as a bridging mono-dentate ligand, while 2-Pbim ligand acts as a chelating bidentate mode to link Cd atoms. The 1D chains are connected by a Bdc ligand with a 2D layer along the *bc* plane, as illustrated in Figure 3. This layer can be reduced to a (4, 4) topology (Figure 4).

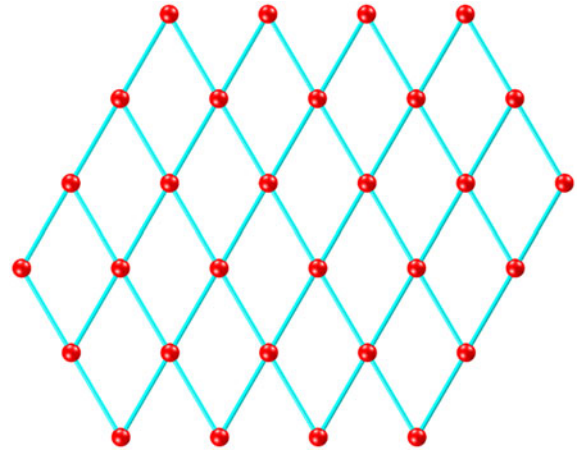

Figure 4. (Colour online) Simplified (4, 4) topology structure of **1**.

Thermal stability analysis

TGA was carried out to examine the thermal stability of complex **1** (Figure 5). The crushed single-crystal sample

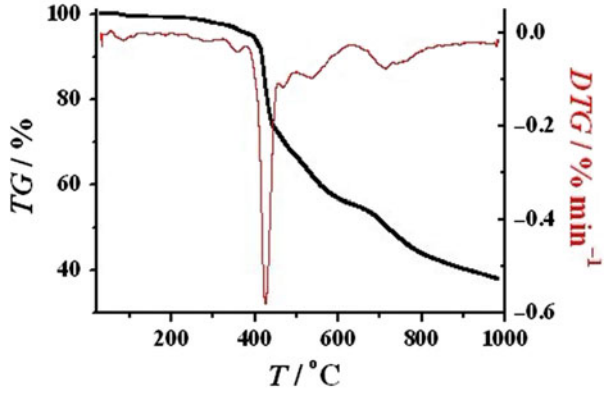

Figure 5. (Colour online) TG-DTG curve of **1.**

was heated up to 1000°C in N_2 at a heating rate of 10°C min^{-1}. The TG/DTG curves for **1** show that it collapsed with a total loss of 75.3% (calcd 76.9%), consistent with the pyrolysis of mixed ligands. The pyrolysis of mixed ligands occurred in the temperature range 100–800°C. The above-mentioned different thermal behaviours may attribute to their structural features, the presence of abundant coordination bonds involving carboxylate ligands and the chelating effect of five-membered rings, which change the bond angles for chelating, resulting in the formation of a rich variety of polymeric structures.

Photoluminescence properties

The emission spectrum of complex **1** in the solid state was investigated at room temperature. Excitation at 365 nm leads to a strong blue fluorescent emission band at 449 and 562 nm for **1**. These emissions are neither metal-to-ligand charge transfer nor ligand-to-metal charge transfer in nature since Cd(II) ions are difficult to be oxidised or to be reduced due to their d^{10} configuration (*21*). For the free H_2Bdc ligand, the emission band at 387 nm ($\lambda_{ex} = 351$ nm) can be assigned to $\pi-\pi^*$ transition. In addition, for the free 2-Pbim, the main emission bands at 503 nm ($\lambda_{ex} = 490$ nm) are assigned to the intraligand $\pi-\pi^*$ transition (*22*). Therefore, we assign the emissions described above for **1** to ligand-to-ligand charge transfer excited states.

In vitro *antitumour activity assay*

The cell growth inhibition rates of complex **1** against four selected tumour cell lines were evaluated by MTT methods, as shown in Figure 6. After incubation of tumour cells and the complex at 10 μM for 48 h under identical experimental conditions, complex **1** and its ligands exhibit different antitumour activity.

As shown in Figure 6, complex **1** displays greater inhibition than the free benzimidazole ligand towards four tumour cell lines. The inhibition rate is 50% or so, which is higher than that of free ligand, 2-Pbim, but lower than that of free ligand, OH-H_2Bdc.

DNA interaction studies

Absorption titrations

The UV–vis absorption spectrum of complex **1** in the absence and presence of increasing amounts of DNA is shown in Figure 7. Complex 1 has two absorption peaks at 258 and 312 nm, which can be assigned to the $\pi \rightarrow \pi^*$ (at 258 nm) and $n \rightarrow \pi^*$ (at 312 nm) transitions of the benzimidazole rings. The titration of DNA induces the hyperchromism of 104.5% and bathochromism of 3 nm (Figure 7) around 258 nm for complex **1**. Such an observation is likely to reflect levels of intercalation of the complex with the DNA base stacks. DNA is a long polynucleotide chain assembled by 5′-deoxynucleotides through phosphodiester bonds, in which its base stacks are inside the duplex DNA. Under physiological conditions, negative phosphates along the DNA backbone are hydrophilic, and base pairs are hydrophobic. The base-stacking forces, hydrogen bonding and electrostatic interactions between negative phosphates and positive sodium or potassium ion can stabilise the double-helical structure of DNA. When the ratio of [DNA]/[complex] increases from 0 to 10, the complex can penetrate into the adenine base stacks of the double-helical DNA, which can cause hydrophobic interaction made up of base-stacking forces and van der Waals force to vary correspondingly, affecting the stability of DNA conformation and unwinding the double-helical structure of DNA and increasing the

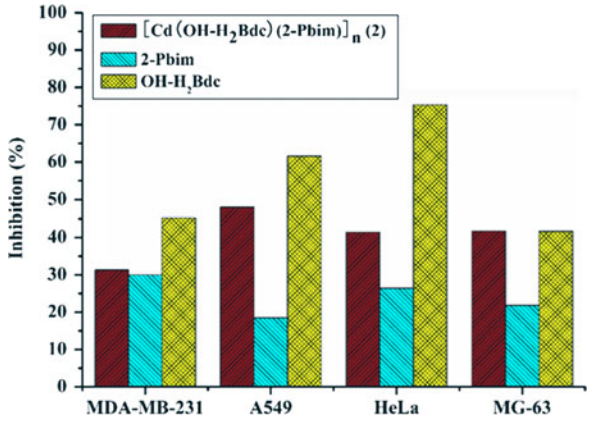

Figure 6. (Colour online) Cytotoxic activity of complex **1** against four human tumour cell lines.

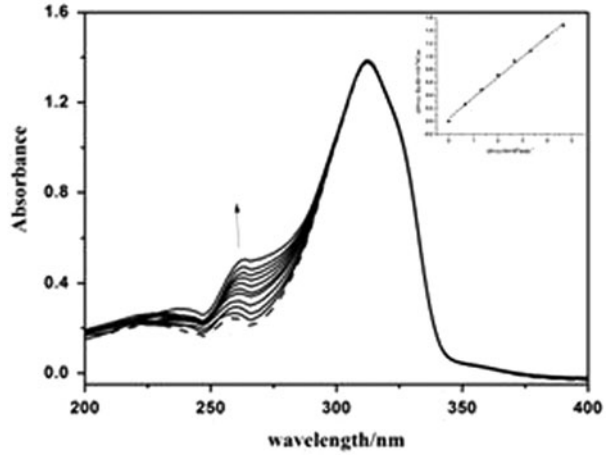

Figure 7. Absorption spectrum of complex **1** in 5 mM Tris buffer (pH 7.35) in the absence and presence of ct-DNA.

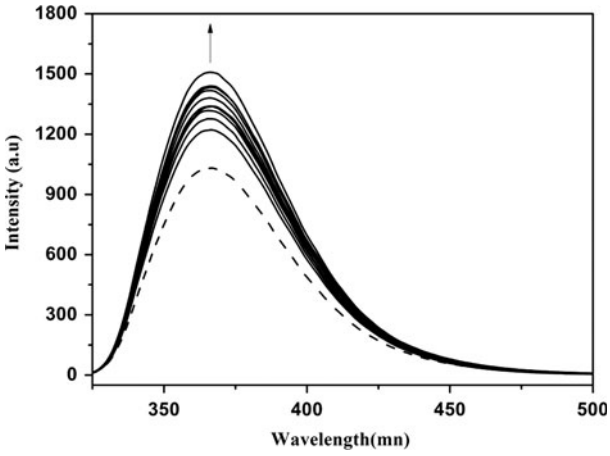

Figure 8. Emission spectrum of complex **1** in 5 mM Tris buffer (pH 7.35) in the absence and presence of ct-DNA.

UV-vis absorption of purine and pyrimidine bases (*23*). On the other hand, the behaviour may result from the association of the compound bound to DNA, which causes damage to hydrogen bonds between aggregates and complexes in solution brought about by the penetration of complexes into the DNA base stacks (*24*, *25*).

To compare quantitatively the binding strength of the complex, the intrinsic binding constants K_b with DNA are determined from the increase of the absorbance with increasing concentrations of DNA using the Equation (*26*):

$$\frac{[\mathrm{DNA}]}{\varepsilon_a - \varepsilon_f} = \frac{[\mathrm{DNA}]}{\varepsilon_b - \varepsilon_f} + \frac{1}{K_b(\varepsilon_b - \varepsilon_f)},$$

where ε_a, ε_f and ε_b are the extinction coefficients of the given, free in solution and fully bound complex, respectively, K_b is the equilibrium binding constant, [DNA] is the DNA concentration in 0.1 M Tris buffer (pH 7.35) containing 5% DMSO. In the plot of [DNA]/($\varepsilon_a - \varepsilon_f$) versus [DNA], a slope of $1/(\varepsilon_b - \varepsilon_f)$ and an intercept of $1/[K_b(\varepsilon_b - \varepsilon_f)]$ are given; the intrinsic binding constants, K_b, can be obtained by the ratio of the slope of the intercept. Complex **1** can interact with the base pairs of the double-helical DNA via an intercalative mode with intrinsic binding constant, K_b, of 2.48×10^6, presenting high DNA-binding affinity.

Fluorescence studies

The fluorescence spectrum for complex **1** in the presence of increasing amounts of DNA is shown in Figure 8. When excited at 312 nm, complex **1** exhibits a fluorescent emission band at 367 nm. Fluorescence intensity gradually increases with the addition of DNA, reaching a maximum at the ratio of [DNA]/[Complex] = 10, at which there are 0.50 times enhancements in the fluorescence intensity compared with those in the absence of DNA.

As shown in Figure 8, emission peaks are observed to increase for complex **1** upon addition of DNA, which also suggests that complex **1** intercalates with the base pair of duplex DNA rather strongly. The fluorescence enhancement has resulted from the fact that fluorescence molecules in the hydrophobic environment between base pairs of double-helical DNA are effectively protected against collision of solvent molecules and energy dissipation with the environmental water and oxygen (*27*, *28*). In general, complex **1** can interact with the base pairs of DNA helix via the combined mode of intercalation and groove binding.

Summary

In summary, we have successfully synthesised the novel coordination polymers endowed with 5-hydroxyisophthalic acid and benzimidazole analogues by the hydrothermal method. In this study, we have attempted to unravel the DNA interactions of the novel mixed–ligand benzimidazole complexes. Based on UV titration and fluorescence titration, the combined mode of intercalation and groove binding for complex **1** is suggested. Complex **1** can interact with the base pairs of the double-helical DNA via an intercalative mode with intrinsic binding constant, K_b, of 2.48×10^6, presenting high DNA-binding affinity.

Supplementary materials

CCDC No. 827563, contains the supplementary crystallographic data. These data can be obtained via the Cambridge Crystallographic Data Centre (deposit@ccdc.cam.ac.uk; http://www.ccdc.cam.ac.uk/deposit).

Funding

We acknowledge financial support by the National Natural Science Foundation of China [grant number 21341005].

References

(1) Hannon, M.J. *Chem. Soc. Rev.* **2007**, *36*, 280–295.
(2) Kelley, S.O.; Barton, J.K. Science **1999**, *283*, 375–381.
(3) Metcalfe, C.; Thomas, J.A. *Chem. Soc. Rev.* **2003**, *32*, 215–224.
(4) Li, Y.P.; Wu, Y.B.; Zhao, J.; Yang, P.J. *Inorg. Biochem.* **2007**, *101*, 283–290.
(5) Su, Y.S.; Lin, M.J.; Sun, M.Ch. *Tetrahedron Lett.* **2005**, *46*, 177–180.
(6) Wang, D.E.; Deng, K.J.; Lv, K.L.; Wang, C.G.; Wen, L.L.; Li, D.F. *CrystEngCommun.* **2009**, *11*, 1442–1450.
(7) Tao, J.; Zhang, Y.; Tong, M.L.; Chen, X.M.; Tan, Y.; Lin, C.L.; Huang, X.; Li, J. *Chem. Commun.* **2002**, 1342–1343.
(8) Ma, C.L.; Han, Y.H.; Li, D.C. *Polyhedron* **2004**, *23*, 1207–1216.
(9) Ye, J.W.; Li, D.; Ye, K.Q.; Liu, Y.; Zhao, Y.F.; Zhang, P.Z. *Anorg. Allg. Chem.* **2008**, *634*, 345–351.

(10) Liu, L.; Zhang, H.; Meng, X.G.; Yin, J.; Li, D.F.; Liu, C.L. *Biomaterials* **2010**, *31*, 1380–1391.
(11) Liu, H.K.; Sadler, P.J. *Acc. Chem. Res.* **2011**, *44*, 349–359.
(12) Yang, Y.; Zeng, M.H.; Zhang, L.J.; Liang, H. *Chin. J. Struct. Chem.* **2009**, *28*, 1671–1676.
(13) Yang, Y.; Zeng, M.H.; Zhang, L.J.; Liang, H.J. *Coord. Chem.* **2009**, *62*, 886–893.
(14) Yang, Y.; Zeng, M.H.; Zhao, X.H.; Liang, H. *Inorg. Chim. Acta* **2009**, *362*, 3065–3068.
(15) Marmur, J. *J. Mol. Biol.* **1961**, *3*, 208–218.
(16) Reichmann, M.E.; Rice, S.A.; Thomas, C.A.; Doty, P. *J. Am. Chem. Soc.* **1954**, *76*, 3047–3053.
(17) Sheldrick, G.M. *SHELXS-97, Program for Crystal Structure Determination*; University of Göttingen: Göttingen, Germany, 1997.
(18) Sheldrick, G.M. *SHELXL-97, Program for Crystal Structure Refinement*; University of Göttingen: Göttingen, Germany, 1997.
(19) Alley, M.C.; Scudiero, D.A.; Monks, A.; Hursey, M.L.; Czerwinski, M.J.; Fine, D.L.; Abbott, B.J.; Mayo, J.G.; Shoemaker, R.H.; Boyd, M.R. *Cancer Res.* **1988**, *48*, 589–601.
(20) Chen, Z.F.; Liu, Y.C.; Liu, L.M.; Wang, H.S.; Qin, S.H.; Wang, B.L.; Bian, H.D.; Yang, B.; Fun, H.K.; Liu, H.G.; Liang, H.; Orvig, C. *Dalton. Trans.* **2009**, 262–272.
(21) Liu, F.Q.; Wang, Q.X.; Jiao, K.; Jian, F.F.; Liu, G.Y.; Li, R. X. *Inorg. Chim. Acta.* **2006**, *359*, 1524–1530.
(22) Zhang, Q.L.; Liu, J.G.; Liu, J.Z.; Li, H.; Yang, Y.; Xu, H.; Chao, H.; Ji, L.N. *Inorg. Chim. Acta.* **2002**, *339*, 34–40.
(23) Wu, S.S.; Zhang, Y.F.; Du, J.F.; Zhang, Q.; Yuan, W.B.; Gu, H.B. *Spectrosc. Spect. Anal.* **2008**, *28*, 374–379.
(24) Liu, J.; Zhang, T.X.; Lu, T.B. J. Inorg Biochem **2002**, *91*, 269–276.
(25) Tu, C.; Wu, X.F.; Liu, Q. *Inorg. Chim. Acta.* **2004**, *357*, 95–102.
(26) Harsh, R.H.; Barton, J.K. *J. Am. Chem. Soc.* **1992**, *114*, 5919–5925.
(27) Cheng, F.X.; Tang, N.; Chen, J.S.; Wang, F.; Chen, L.H. *Inorg. Chem. Commun.* **2010**, *13*, 757–761.
(28) Li, J.H.; Wang, J.T.; Mao, Z.W.; Ji, L.N. *Inorg. Chem. Commun.* **2008**, *11*, 865–868.